PERGAMON

Electrochimica Acta 44 (1999) 3977–3987

ELECTROCHIMICA Acta

Effect of Co content on the kinetic properties of the $MlNi_{4.3-X}Co_XAl_{0.7}$ hydride electrodes

Hongge Pan*, Jianxin Ma, Chunsheng Wang, C.P. Chen, Q.D. Wang

Department of Materials Science and Engineering, Zhejiang University, Hangzhou 310027, People's Republic of China

Received 27 October 1998; received in revised form 3 March 1999

Abstract

By means of linear polarization, Tafel polarization and galvanostatic discharge methods, the kinetic properties of $MlNi_{4.3-X}Co_XAl_{0.7}$ ($X=0.0$, 0.3, 0.5, 0.7, 0.9, 1.1 and 1.3) hydride electrodes, including high rate dischargeability HRD, exchange current density I_0, limiting current density I_L, the symmetry factor β, and the apparent diffusion coefficient of hydrogen in the α phase D_α have been studied systematically. The results show that the HRD of the electrode with high Co content is lower than that with low Co content. For the $MlNi_{4.3-X}Co_XAl_{0.7}$ hydride electrodes, with Co content increasing from 0.0 to 1.3, the values of I_0, I_L, β and D_α decreased from 395 to 33 mA/g, 2263 to 308 mA/g, 0.85 to 0.43, 1.42×10^{-10} to 2.1×10^{-11} cm^2/s, respectively. In order to calculate the electrochemical polarization η_e and concentration polarization η_c based on anodic polarization curve, the experimental anodic polarization curve should be divided into three regions to discuss according to discharge current density I_d, namely, $I_d < I_P$, $I_P < I_d < I_f$, and $I_d > I_f$. The calculation of η_e and η_c should use different formula in different regions. When discharge current density I_d is smaller than I_p, the traditional equation used to calculate the electrochemical overpotential can not be used, when I_p is between I_p and I_f, both equations used to calculate the electrochemical overpotential and concentration overpotential can be used, and when I_d is larger than I_f, because there exists absorption and adsorption of hydrogen, the traditional equation used to calculate concentration overpotential can not be used in the system of hydride electrodes.

1. Introduction

Metal hydrides have been used as negative electrodes of nickel/metal hydride batteries because of their high energy density, high charge and high dischargeability, long charge–discharge cycle life and environmental compatibility [1–6]. The performance of a hydride electrode is determined by the thermodynamic properties, such as plateau pressure P_{plat}, the hydrogen concentration of α phase and β phase at interface between α and β phase $C_{\alpha\beta}$, $C_{\beta\alpha}$ at P_{eq} and the kinetic properties, i.e. exchange current density I_0, diffusion coefficient of hydrogen in the α phase D_α and the geometric parameter r_0.

The hydrogen desorption process during discharge is composed of several partial steps in the alkaline solution [2,3]:

1. nucleation and growth of α phase from β phase.
2. diffusion of hydrogen from α phase through the oxide film to the near-surface region of the particle.
3. transfer of the hydrogen from the absorbed site in

* Corresponding author. Tel.: +86-571-795-1406; fax: +86-571-795-1152.

E-mail address: pan_hg@mail.hz.zj.cn (H. Pan)

0013-4686/99/$ - see front matter
PII: S0013-4686(99)00116-4

Nomenclature

C_S	the hydrogen concentration of α phase on the near surface of a particle (mol/cm^3)
$C_{\alpha\beta}$,$C_{\beta\alpha}$	the hydrogen concentration of the α or β phase equilibrating with P_{eq} at the interface between α and β phase (mol/cm^3)
C_α	real hydrogen of the α phase at the interface between the α and β phase (mol/cm^3)
D_α	apparent diffusion coefficient of hydrogen in the α phase including hydrogen diffusion through the oxide film on the surface and transfer from absorbed sites to adsorbed sites
F	Faraday constant, 96547 (J/V mol)
I_d	discharge current density (mA/g)
I_0	exchange current density (mA/g)
I_L	limiting current density (mA/g)
I_P	peak discharge current (mA/g)
I_f	critical point current (mA/g)
k	rate constant (mol/g s)
K	equilibrium constant (-)
N_m	the total number of interstitial sites available for hydrogen per unit volume of the host metal
Q_i	discharge capacity at discharge current density I_d with cutoff voltage 0.6 V (mA h/g)
Q_d	discharge capacity (mA h/g)
Q_{max}	maximum discharge capacity (mA h/g)
r_0	average radius of the particle (cm)
r_α	radius of unreacted β phase in discharge process (cm)
R	gas constant, 8.31 (J/mol K)
β	symmetry factor (-)
ρ	density (g/cm^3)
η	overall overpotential (V)
η_e	electrochemical overpotential (V)
η_c	concentration overpotential (V)

the near surface to the adsorbed site on the electrode surface.

$$MH_{abs} \underset{k_{-2}}{\overset{k_2}{\Leftrightarrow}} MH_{ads}. \quad (1)$$

4. electrochemical oxidation of hydrogen, namely, occurring electrochemical reaction at the electrode surfaces.

$$MH_{ads} + OH^- \underset{k_{-3}}{\overset{k_3}{\Leftrightarrow}} M + H_2O + e. \quad (2)$$

Two classes of metal hydride alloys currently being developed are AB_5 type intermetallic compounds, where A represents rare earth elements and B includes any of late transition or p-shell elements [4–5] and AB_2 type Laves phases, where A and B denote early transition elements [6]. Although the AB_2 alloys are reported to exhibit higher specific energy than the AB_5 alloys, state-of-the-art commercial Ni–MH batteries predominately use AB_5 alloys because of their better overall electrochemical properties.

$LaNi_5$ alloy activates rather easily and absorbs and desorbs a large amount of hydrogen with good charge and discharge kinetics as discovered by Van Vucht et al. [7] in the late 1960s. However, the storage capacity of this alloy declined rapidly during charge and discharge cycles as the alloy decrepitates and transforms to $La(OH)_3$ and nickel. A breakthrough was made by Willems and Buschow [4], who discovered that partial substitution of Ni by Co was very effective to enhance the cycle life of $LaNi_5$ alloy. Since then, many works have been done in investigating the influence of Co on the cycle life of $LaNi_5$ based alloys [8–17]. Up to now, cobalt has been thought to be indispensable for stable AB_5 type battery electrodes. In this paper, the effect of Co on the electrochemical kinetics properties of $MlNi_{4.3-X}Co_XAl_{0.7}$ ($X=0.0$, 0.3, 0.5, 0.7, 0.9, 1.1 and 1.3) hydride electrodes, including high-rate dischargeability HRD, exchange current density I_0, limiting current density I_L, the symmetry factor β and the apparent diffusion coefficient of hydrogen in the α phase D_α have been investigated systematically.

2. Experimental

Hydrogen storage alloys of nominal composition

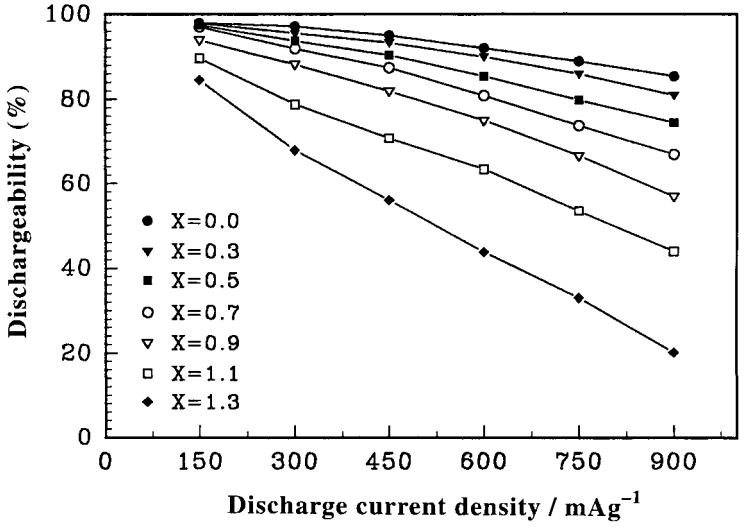

Fig. 1. High rate dischargeability HRD of $MlNi_{4.3-X}Co_XAl_{0.7}$ hydride electrodes.

$MlNi_{4.3-X}Co_XAl_{0.7}$ ($X=0.0$, 0.3, 0.5. 0.7, 0.9, 1.1, 1.3), were prepared by arc melting under an argon atmosphere. The Ml denoted as lanthanum-rich misch metal, which composed of 64.6 w/o La, 5.89 w/o Ce, 26 w/o Pr and 2.24 w/o Nd. The purity of the other metals is at least 99.9 wt%. The ingots were turned over and remelted five times for homogenization, and then the ingots after melting were mechanically pulverized and ground into fine powders with an average size of 40 μm for use as electrode materials.

The metal hydride electrode was made by first mixing 0.5 g of alloy powder with 0.2 g of carbonyl nickel powder. Three percent PVA solution was added to the mixture as binder. The mixture was cold pressed onto a Ni mesh under pressure of 20 MPa. The effective surface area of the electrode was 1.5×1.5 cm^2 and the thickness of the electrode was about 1.5 mm.

The electrochemical cell for electrochemical measurement consisted of the working electrode (metal hydride electrode), the counterelectrode ($NiOOH/Ni(OH)_2$ electrode), and the reference electrode (Hg/HgO electrode). The Hg/HgO electrode was equipped with Luggin tube to reduce the IR drop during the polarization and electrochemical impedance spectroscopy measurements. The electrolyte was a 6 M KOH solution and the temperature was controlled at 25 ± 1°C. The discharge capacity of the electrode was determined by the galvanostatic method. The cutoff voltage for discharging was fixed at −600 mV with respect to the Hg/HgO electrode. Before polarization and electrochemical impedance spectroscopy measurements, the hydrogen storage hydride electrode was activated completely (20 cycles). The average particle size of hydride electrode after activation was determined by scanning electron microscopy (SEM). In order to investigate high rate dischargeability, the discharge capacity at different discharge current densities was measured.

3. Results and discussion

3.1. Effect of Co content on the high rate dischargeability

One main parameter characterizing the practical application of hydride electrodes is the high rate dischargeability (HRD). The HRD can be defined as the ratio of the discharge capacity Q_i with cutoff voltage 0.6 V at the discharge current density I_d to the maximum discharge capacity Q_{max}.

$$HRD = (Q_i/Q_{max}) \times 100\%. \quad (3)$$

Fig. 1 shows the high rate dischargeability HRD dependence of Co content in the $MlNi_{4.3-X}Co_XAl_{0.7}$ hydride electrodes. The HRD decreases rapidly with the increase in the Co content. For example, the HRD of $MlNi_{4.3}Al_{0.7}$ hydride electrode is three times higher than that of $MlNi_{3.0}Co_{1.3}Al_{0.7}$ hydride electrode at the discharge current density of 900 mA/g.

After activation, the high rate dischargeability HRD can be expressed as [2]:

$$HRD = 1 - \left(1/\left(\frac{3FD_\alpha C_{\alpha\beta}}{I_d \rho r_0^2}\right) \times \left[1 - \frac{I_d}{I_0}\exp\left(-\frac{\beta F}{RT}\eta\right) + 1\right]\right)^3. \quad (4)$$

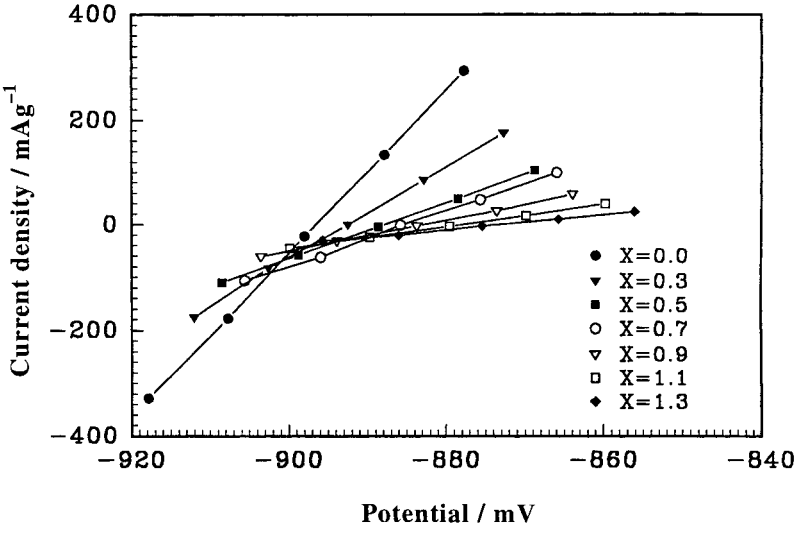

Fig. 2. Linear polarization curves of $MlNi_{4.3-X}Co_XAl_{0.7}$ hydride electrodes.

It is obvious that the HRD is mainly determined by kinetic properties, such as exchange current density I_0, the apparent diffusion coefficient of hydrogen in α phase (including hydrogen diffusion through the oxidation film on the surface of particles) D_α, and thermodynamic properties, such as $C_{\beta\alpha}$ and $C_{\alpha\beta}$. If only kinetic parameters are considered, the HRD is mainly determined by the polarization controlling step. The effect of Co on the I_0, I_L in $MlNi_{4.3}Al_{0.7}$ hydride electrodes are discussed in following sections.

3.2. Effect of Co content on the exchange current density I_0

In order to determine the exchange current density I_0 and the polarization resistance, the linear polarization experiment was conducted at 50% state of discharge (SOD) and scanning rate 5 mV/s. The results are presented in Fig. 2. It revealed that the polarization increased with the increase in Co content in the $MlNi_{4.3-X}Co_XAl_{0.7}$ hydride electrodes. The exchange current density I_0 can be calculated according to the following formula [18]:

$$I_0 = \frac{I_d RT}{F\eta}. \quad (5)$$

The exchange current densities I_0 calculated by Eq. (5) are listed in Table 1. The exchange current density I_0 decreases from 395 mA/g for $X=0.0$ to 33 mA/g for $X=1.3$, respectively. This means that, with the increase in Co content X, the I_0 decreases seriously. This result is similar to that by Iwakura et al. [17].

Table 1
The exchange current density I_0, limiting current density I_L, symmetry β, and the apparent diffusion coefficient of hydrogen D_α in the α phase in $MlNi_{4.3-X}Co_XAl_{0.7}$ hydride electrodes

X in $MlNi_{4.3-X}Co_XAl_{0.7}$	I_0 (mA/g)	I_L (mA/g)	β	D_α (cm^2/s)
0.0	395	2263	0.85	1.4×10^{-10}
0.3	233	1295	0.74	9.8×10^{-11}
0.5	147	1053	0.67	8.1×10^{-11}
0.7	91	805	0.64	5.4×10^{-11}
0.9	75	477	0.61	4.1×10^{-11}
1.1	45	390	0.57	3.2×10^{-11}
1.3	33	308	0.43	2.1×10^{-11}

3.3. Effect of Co content on the diffusion coefficient of hydrogen

During galvanostatic discharge, the apparent diffusion coefficient of hydrogen in α phase (including hydrogen diffusion through the oxidation film on the surface of particles) can be calculated by the following equation [19]:

$$D_\alpha = \frac{r_0^2 I_d}{15(Q_0 - \tau I_d)}, \quad (6)$$

where Q_0, I_d, τ, and r_0 is the initial specific capacity, the discharge current density, transition time, i.e. the time when the hydrogen surface concentration is zero, and the average particle radius, respectively.

The calculated D_α according to Eq. (6) (the r_0 determined by SEM) are also presented in Table 1. It is obvious that the apparent diffusion coefficient of

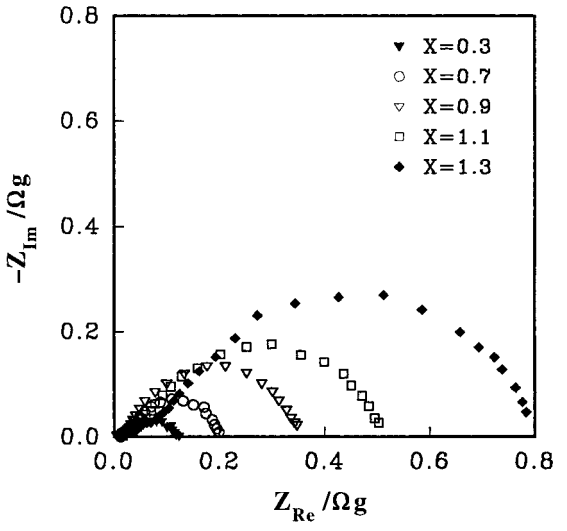

Fig. 3. Electrochemical impedance spectra of the $MlNi_{4.3-X}Co_XAl_{0.7}$ electrodes at $X=0.3$, 0.7, 0.9, 1.1 and 1.3.

hydrogen in α phase D_α decreases with the increase in Co content in the $MlNi_{4.3-X}Co_XAl_{0.7}$ hydride electrodes. For example, the D_α at $X=0.0$ is nine times higher compared with that at $X=1.3$. This result also can be confirmed by the results of electrochemical impedance spectra. Fig. 3 shows the electrochemical impedance spectra of in the $MlNi_{4.3-X}Co_XAl_{0.7}$ hydride electrodes at $X=0.3$, 0.7, 0.9, 1.1 and 1.3. According to Wang's mathematical model [20], the low frequency semicircle in the electrochemical impedance spectra is attributed to the hydrogen diffusion in the α phase. The radius of this semicircle increases with increasing Co content meaning that the apparent diffusion coefficient of hydrogen in α phase D_α decreases with an increase of Co content X in $MlNi_{4.3-X}Co_XAl_{0.7}$ hydride electrodes.

3.4. Effect of Co content on the anodic polarization

3.4.1. Limiting current density I_L

Fig. 4 shows that the anodic current in response to the overpotential of the $MlNi_{4.3-X}Co_XAl_{0.7}$ hydride electrodes at 50% SOD. The overall overpotential at same discharge current density increases with increasing Co content X. The corresponding limiting current density I_L at different X is listed in Table 1. The limiting current density I_L decreases dramatically with the increase in X, i.e. the limiting current density I_L at $X=0.0$ is about eight times higher compared with that at $X=1.3$ in the $MlNi_{4.3-X}Co_XAl_{0.7}$ hydride electrodes.

3.4.2. Calculation of the η_e, η_c and η_e/η_c

It is well known that the overall overpotential η can be expressed as

$$\eta = \eta_e + \eta_c. \tag{7}$$

The η_e is the electrochemical polarization and η_c is the concentration (diffusion) polarization.

The η_e and η_c can be calculated by

$$\eta_e = \frac{RT}{\beta F} ln \frac{I_d}{I_0} \tag{8}$$

$$\eta_c = \frac{RT}{\beta F} ln \frac{I_L}{I_L - I_d}. \tag{9}$$

Substituting Eqs. (8) and (9) into Eq. (7), the overall

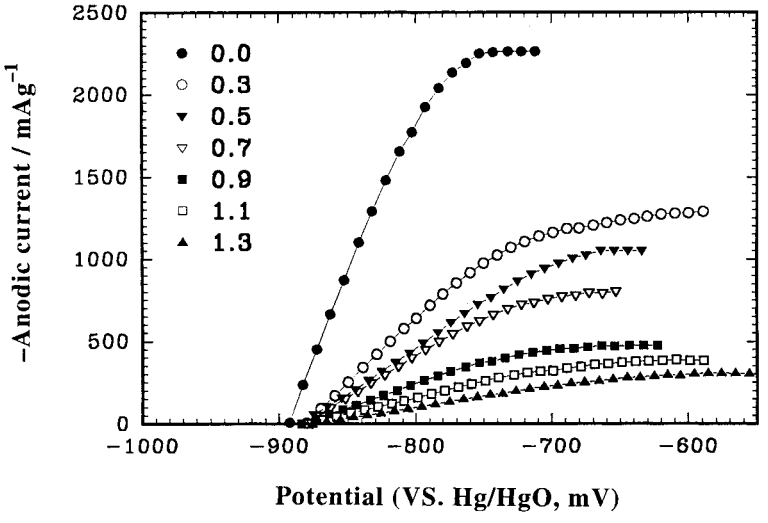

Fig. 4. Anodic polarization of $MlNi_{4.3-X}Co_XAl_{0.7}$ hydride electrodes.

overpotential η can be expressed by

$$\eta = \frac{RT}{\beta F} ln\left(\frac{I_d}{I_0}\right) + \frac{RT}{\beta F} ln\left(\frac{I_L}{I_L - I_d}\right). \quad (10)$$

If the η, I_L and β are known, the η_e also can be calculated by

$$\eta_e = \eta - \frac{RT}{\beta F} ln\left(\frac{I_L}{I_L - I_d}\right). \quad (11)$$

And if the η, I_0 and β are available, the η_c also can be calculated by

$$\eta_c = \eta - \frac{RT}{\beta F} ln\left(\frac{I_d}{I_0}\right). \quad (12)$$

Rewriting Eq. (10), the following expression can be obtained:

$$\eta = \frac{RT}{\beta F} ln\left(\frac{I_L}{I_0}\right) + \frac{RT}{\beta F} ln\left(\frac{I_d}{I_L - I_d}\right). \quad (13)$$

According to Eq. (13), a plot of η vs. $\ln(I_d/I_L - I_d)$ should produce a straight line with its slope being $RT/\beta F$. Therefore, symmetry factor in the oxidation direction can be calculated from data of I_L and T. The calculated β is also listed in Table 1. It can be seen that the symmetry factor in the oxidation direction β decreases with increasing Co content X.

In order to discuss polarization controlling steps at different discharge current densities I_d, the ratio of the electrochemical polarization η_e to the concentration (diffusion) polarization η_c, η_e/η_c should be calculated [2]. According to Eq. (7–9) the η_e/η_c can be obtained:

$$\frac{\eta_e}{\eta_c} = \frac{(RT/\beta F) ln(I_d/I_0)}{(RT/\beta F) ln(I_L/(I_L - I_d))} \quad (14)$$

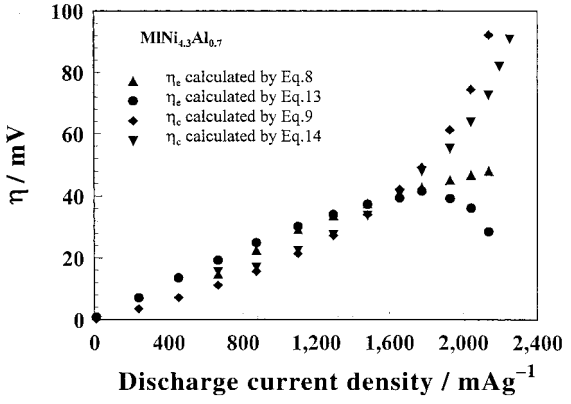

Fig. 5. Electrochemical overpotential η_e and concentration overpotential η_c in $MlNi_{4.3}Al_{0.7}$ hydride electrodes calculated by different expressions.

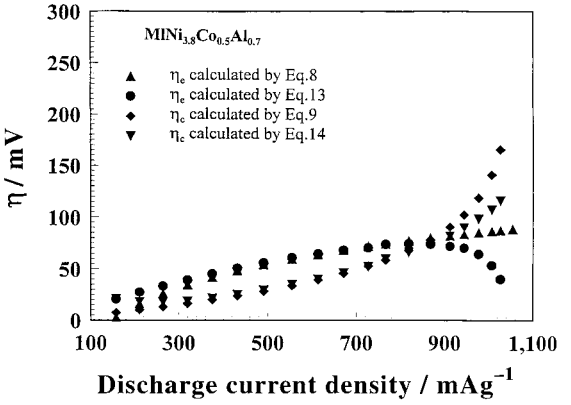

Fig. 6. Electrochemical overpotential η_e and concentration overpotential η_c in $MlNi_{3.8}Co_{0.5}Al_{0.7}$ hydride electrodes calculated by different expressions.

or

$$\frac{\eta_e}{\eta_c} = \frac{\eta - (RT/\beta F) ln(I_L/(I_L - I_d))}{(RT/\beta F) ln(I_L/(I_L - I_d))} \quad (15)$$

or

$$\frac{\eta_e}{\eta_c} = \frac{(RT/\beta F) ln(I_d/I_0)}{\eta - (RT/\beta F) ln(I_d/I_0)}. \quad (16)$$

Yang et al. [21] used Eq. (8) and (9)to calculate the η_e and η_c in the whole anodic polarization process. Like Yang et al. the electrochemical overpotential η_e calculated by Eq. (8) and concentration overpotential η_c calculated by Eq. (9) are shown in Fig. 5, Figs. 6 and Fig. 7 (up triangle for η_e and rhomb for η_c) at $X = 0.0$, 0.5, 1.3 in $MlNi_{4.3-X}Co_XAl_{0.7}$ hydride electrodes, respectively. The corresponding ratio of η_e/η_c dependence of discharge current density I_d at $X = 0.0$,

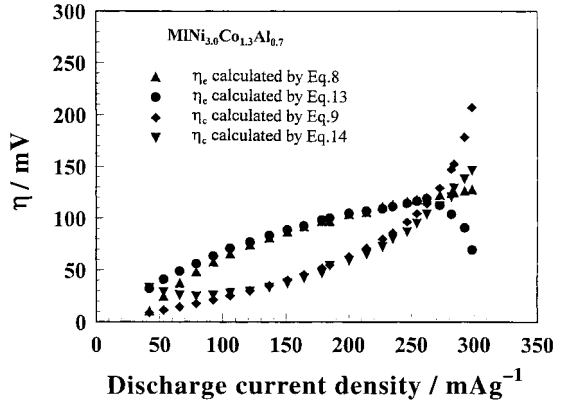

Fig. 7. Electrochemical overpotential η_e and concentration overpotential η_c in $MlNi_{3.0}Co_{1.3}Al_{0.7}$ hydride electrodes calculated by different expressions.

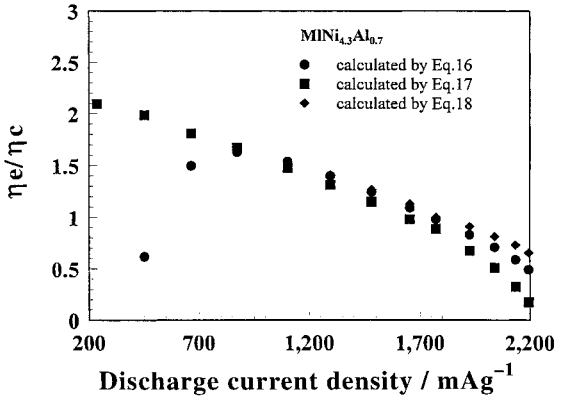

Fig. 8. The ratio of electrochemical overpotential η_e to concentration overpotential η_c in $MlNi_{4.3}Al_{0.7}$ hydride electrodes calculated by different expressions.

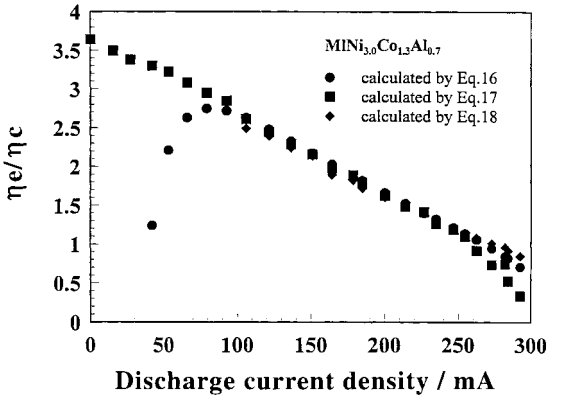

Fig. 10. The ratio of electrochemical overpotential η_e to concentration overpotential η_c in $MlNi_{3.0}Co_{1.3}Al_{0.7}$ hydride electrodes calculated by different expressions.

0.5, 1.3 are presented in Figs. 8–10 (indicated by circle). The ratio of η_e/η_c increases with an increasing discharge current density initially, passes through a maximum $(\eta_e/\eta_c)_{max}$ at a certain discharge current density I_p and then decreases with increasing discharge current density.

Differentiating Eq. (14) with respect to discharge current density I_d and letting $d(\eta_e/\eta_c)/dI_d = 0$, the $(\eta_e/\eta_c)_{max}$ and the approximate peak current density of I_d corresponding to $(\eta_e/\eta_c)_{max}$ can be obtained:

$$\left(\frac{\eta_e}{\eta_c}\right)_{max} = \frac{I_L}{I_P} - 1 \tag{17}$$

$$I_P \approx \frac{-2I_L^2 - I_L I_0 + \sqrt{4I_L^4 + 4I_L^3 I_0 + 17I_L^2 I_0^2}}{2I_0}. \tag{18}$$

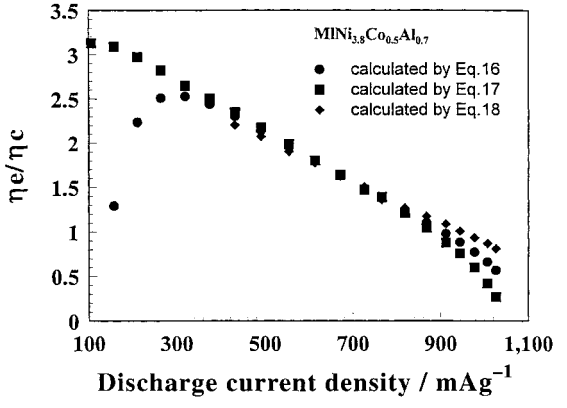

Fig. 9. The ratio of electrochemical overpotential η_e to concentration overpotential η_c in $MlNi_{3.8}Co_{0.5}Al_{0.7}$ hydride electrodes calculated by different expressions.

Differentiating the I_P with respect to I_L and I_0, respectively, the following results can be obtained:

$$\frac{\partial I_P}{\partial I_0} > 0 \tag{19}$$

$$\frac{\partial I_P}{\partial I_L} > 0 \tag{20}$$

$$\frac{\partial I_P}{\partial I_0} - \frac{\partial I_P}{\partial I_L} > 0. \tag{21}$$

It can be seen that, from Eqs. (18)–(21), the peak current density I_p is a function of exchange current density I_0 and limiting current density I_L, and the I_P increases with the increase in the I_L and I_0, but the effect of I_0 is larger than I_L. Fig. 11 presents the peak current density at different Co content in $MlNi_{4.3-X}Co_XAl_{0.7}$ hydride electrodes.

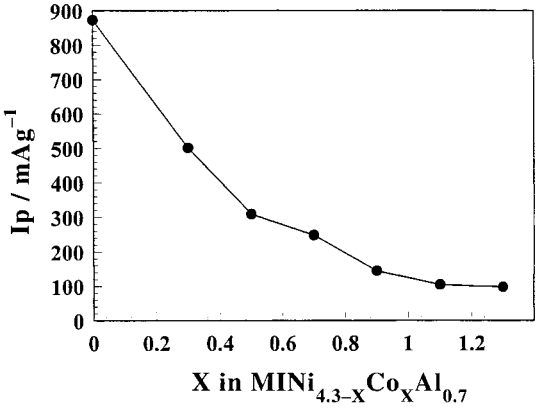

Fig. 11. Peak current density I_P dependence of Co content in $MlNi_{4.3-X}Co_XAl_{0.7}$ hydride electrodes.

Generally speaking, Eqs. (9) and (11) can also be used to calculate the η_c and η_e, where the overall overpotential η used to calculate the η_e is an experimental value during anodic polarization. The η_e and η_c vs. I_d calculated by this means at $X=0.0$, 0.5, 1.3 in the $MlNi_{4.3-X}Co_XAl_{0.7}$ hydride electrodes are also shown in Figs. 5–7 (circle for η_e and rhomb for η_c) respectively, and the corresponding η_e/η_c (calculated by Eq. (15)) at $X=0.0$, 0.5, 1.3 are shown in Fig. 8, Fig. 9 and Fig. 10 (indicated by square). It can be seen that, when I_d is larger than I_P, but smaller than I_f (see next paragraph), η_e, η_c, and η_e/η_c calculated by Eqs. (9), (11) and (15) are similar to those calculated by Eqs. (8), (9) and (14), and when I_d is smaller than I_P, η_e, η_c and η_e/η_c calculated by Eqs. (8), (9) and (14) are smaller than those calculated by Eqs. (9), (11) and (15). Furthermore, this difference becomes much larger with the decreasing discharge current density. Theoretically speaking, Eqs. (9), (11) and (15) can be used to calculate the η_e, η_c and η_e/η_c in any condition as long as the SOD is constant, but when Eqs. (8), (9) and (14) are used, the condition $\eta \gg RT/\beta F$ should be met. Therefore, Eqs. (8), (9) and (14) cannot be used to calculate the η_e and η_c when $I_d < I_P$. The peak current or critical point current I_p can be used to determine which formula should be used to calculate the η_e, η_c and η_e/η_c. This conclusion also can be confirmed by Fig. 12. The overall overpotential calculated by Eqs. (8), (9) and (14) is smaller than the experimental value when $I_d < I_P$, i.e. $I_d < 873$ mA/g at $X=0.0$ in $MlNi_{4.3-X}Co_XAl_{0.7}$ hydride electrodes. So Yang et al. [21] use Eqs. (8) and (9) to calculate the electrochemical overpotential η_e and concentration overpotential η_c is incorrect when I_d is not large enough. Critical point current I_P calculated by Eq. (18) is about 120, 185 and 231 mA/g for alloy B, C and D, respectively, in Yang's paper.

When the discharge current density is close to the limiting current density I_L, it can be seen from Figs. 5–7 (circle) that the η_e calculated by Eq. (11) increases with the increase in the discharge current density, passes through a maximum η_{emax}, and then decreases. This result is unreasonable because the larger the I_d, the higher the η_e. Therefore, Eq. (9) cannot be used to calculate the concentration overpotential η_c. When the discharge current density I_d is very large, i.e. $I_d \rightarrow I_L$, the exchange current density I_0 is constant during the anodic polarization, so the η_e can be calculated by Eq. (8) and η_c can be obtained by experimental value of η minus that of η_e calculated by Eq. (8). The calculated η_e and η_c by these means are also shown in Fig. 5–7 (up triangle for η_e and down triangle for η_c) and the η_e/η_c in Figs. 8–10 (indicated by rhomb). It can be seen that, from Fig. 8–10, when $\eta_e < \eta_{emax}$, the η_e calculated by Eq. 11 is equal to that calculated by Eq. 8. Therefore, a critical point I_f (the discharge current density I_f corresponding to $\eta_e=\eta_{emax}$) also exists. When $I_P < I_d < I_f$, Eq. (9), (11) and (15) can be used to calculate the η_e, η_c and η_e/η_c, but when $I_d > I_f$, Eq. (8), (12) and (16) should be used. Fig. 13 shows the value of I_f at $X=0.0$, 0.3, 0.5, 0.7, 0.9, 1.1 and 1.3 in $MlNi_{4.3-X}Co_XAl_{0.7}$ hydride electrodes. It reveals that the I_f decreases with the increase in Co content.

Eq. (9) just can be used to calculate the concentration overpotential η_c, in which there exists no absorption and adsorption of hydrogen. When the absorption and adsorption process exists, and $\eta \gg RT/\beta F$, the overall overpotential can be expressed as [22]:

$$\eta = \frac{RT}{\beta F} ln \frac{I_d}{I_0} + \frac{RT}{\beta F} ln \frac{\vartheta_0}{\vartheta}, \tag{22}$$

where

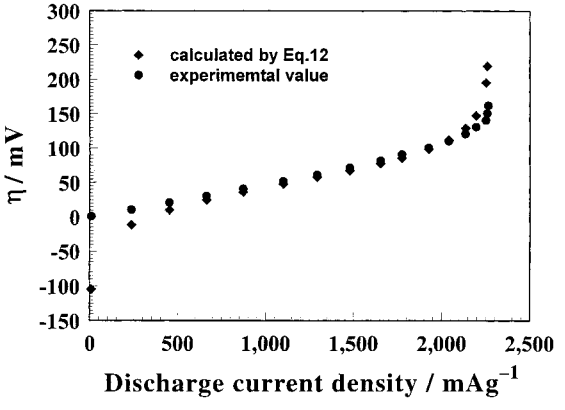

Fig. 12. Comparison of the experimental η (circle) with that calculated by Eq. 15 (rhomb) in $MlNi_{4.3}Al_{0.7}$ hydride electrodes.

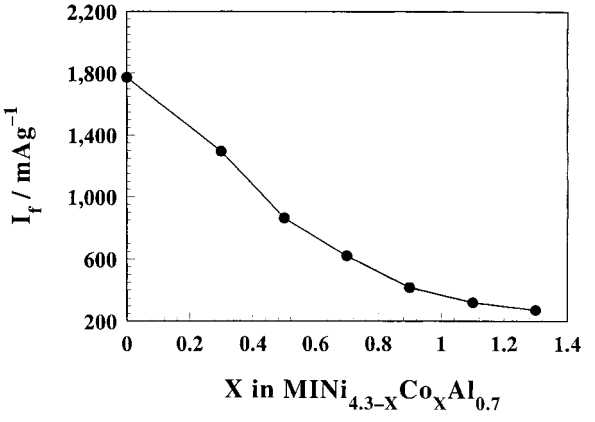

Fig. 13. Critical point current density I_f dependence of Co content in $MlNi_{4.3-X}Co_XAl_{0.7}$ hydride electrodes.

$$\theta_0 = \frac{k_2 C_\alpha}{(k_2 - k_{-2})C_\alpha + k_{-2}N_m} \quad (23)$$

$$\theta = \frac{k_2 C_S - (I_d/F)N_m}{(k_2 - k_{-2})C_S + k_{-2}N_m}. \quad (24)$$

The near surface concentration of hydrogen in the α phase C_S can be expressed as [2]:

$$C_S = C_\alpha - \frac{I_d r_0^2 \rho}{3D_\alpha F}\left(\frac{r_0}{r_\alpha} - 1\right). \quad (25)$$

Letting $C_S = 0$ in Eq. (25), the diffusion limiting current density I_{LD} can be obtained:

$$I_{LD} = \frac{3D_\alpha F C_\alpha}{\rho r_0^2((r_0/r_\alpha) - 1)}. \quad (26)$$

Substituting Eq. (26) into Eq. (25), the C_S can be rewritten as:

$$C_S = C_\alpha\left(1 - \frac{I_d}{I_{LD}}\right). \quad (27)$$

The limiting current density can be written as

$$I_L = \frac{Fk_2 C_S}{N_m}. \quad (28)$$

Substituting Eq. (27) into Eq. (28), the following relationship can be rewritten as:

$$\frac{1}{I_L} = \frac{1}{I_{LD}} - \frac{N_m}{Fk_2 C_\alpha}. \quad (29)$$

Substituting Eq. (29) into Eq. (27), the relationship between C_S and I_L can be rewritten as

$$C_S = C_\alpha\left(1 - \left(\frac{1}{I_L} + \frac{N_m}{Fk_2 C_\alpha}\right)I_d\right). \quad (30)$$

Combining Eqs (22)–(24), and Eq. (30), the overall overpotential can be expressed as

$$\eta = \frac{RT}{\beta F} ln \frac{I_d}{I_0} + \frac{RT}{\beta F} ln \frac{I_L}{I_L - I_d} - \frac{RT}{\beta F} ln\left(\frac{1}{1 - (k_2 - k_{-2})C_\alpha / ((k_2 - k_{-2})C_\alpha + k_{-2}N_m)\left(\frac{I_d}{I_L} + \frac{I_L N_m}{Fk_2 C_\alpha}\right)}\right). \quad (31)$$

When $I_d \ll I_L$, the absorption and adsorption of hydrogen (the third term on the right side in Eq. (31)) can be neglected, then Eq. (31) can be simplified as Eq. (10), but, with the increase in I_d, the concentration overpotential η_c calculated by Eq. (10) will deviate from the real value and the Eq. (31) or Eq. (8) and Eq. (12) should be used.

When the discharge current density is middle ($I_p <$ $I_d < I_f$), it can be seen that, from Figs. 5–10, all three means mentioned above can be used to calculate the η_e, η_c and η_e/η_c. The calculated η_e, η_c, and η_e/η_c fit very well.

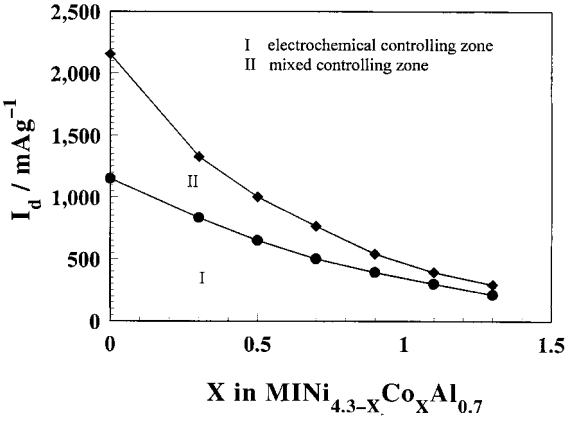

Fig. 14. The electrochemical controlling zone and mixed controlling zone dependence of Co content in $MlNi_{4.3-X}Co_XAl_{0.7}$ hydride electrodes.

3.4.3. Effect of Co content on the η_e, η_c and η_e/η_c

It can be seen that, from Fig. 5–7, the η_e and η_c increase dramatically with increasing Co content in $MlNi_{4.3-X}Co_XAl_{0.7}$ hydride electrodes at same discharge current density. This result can be attributed to the decreases of exchange current density I_0 and limiting current density I_L with increasing Co content.

The ratio of η_e/η_c can be used as criterium to determine the rate-controlling step. The electrochemical reaction is the rate-controlling step when η_e/η_c is higher than 1.5, the hydrogen diffusion is the rate-controlling step when η_e/η_c is smaller than 0.5, and it is a mixed controlling process when η_e/η_c is between 0.5 and 1.5 [2].

Fig. 14 shows the electrochemical controlling zone and mixed controlling zone dependence of Co content. It can be seen that the rate-controlling step gradually changes from an electrochemical controlling step to a mixed controlling step with the increase in discharge current density in $MlNi_{4.3-X}Co_XAl_{0.7}$ hydride electrodes, and more than half of the total polarization process (electrochemical controlling step + mixed controlling step + hydrogen diffusion step) is occupied by electrochemical reaction. Furthermore, the ratio of

electrochemical controlling step to total polarization process becomes larger with the increase in Co content.

Necessarily, Ni was partially substituted by Co in the alloys to enhance the cycle life of $LaNi_5$-based alloy electrodes, but the Co substitution degrades the kinetic properties. According to our results mentioned above, when discharge current is small, the rate-controlling step is an electrochemical reaction, so some methods to enhance the exchange current I_0 should be introduced, i.e. introducing nonstoichiometry [18] or adding the materials possessing high catalytic activity such as Co–Mo alloy [23]. When discharge current is large enough, the rate is controlled by electrochemical reaction and diffusion of hydrogen. Some methods should be introduced to improve the exchange current density I_0 and diffusion coefficient of hydrogen D_α in the α phase, for example, introducing pretreatment by alkaline solution or alkaline solution containing borohydride [24,25].

4. Conclusions

In this paper, the kinetic properties of $MlNi_{4.3-X}Co_XAl_{0.7}$ hydride electrodes have been investigated in great detail. The results show that the exchange current density I_0 and limiting current density I_L decrease from 395 mA/g ($X=0$) to 35 mA/g ($X=1.3$) and from 2263 mA/g ($X=0$) to 308 mA/g in the $MmNi_{4.3-X}Co_XAl_{0.7}$ hydride electrode, respectively, and the diffusion coefficient of hydrogen at $X=0.0$ is much lower than that at $X=0$ in the hydride electrodes. The high rate dischargeability decreases linearly with the increase in Co content. In order to calculate the electrochemical polarization η_e and concentration polarization η_c based on anodic polarization curve, the experimental anodic polarization curve should be divided into three regions to discuss according to discharge current density I_d, namely, $I_d < I_p$, $I_p < I_d < I_f$ and $I_d > I_f$. The calculation of η_e and η_c should use different formula in different regions. When discharge current density I_d is smaller than I_p, the traditional equation used to calculate the electrochemical overpotential cannot be used, and when I_p is between I_p and I_f, both equations used to calculate the electrochemical overpotential and concentration overpotential can be used, and when I_d is larger than I_f, because there exists absorption and adsorption of hydrogen, the traditional equation used to calculate concentration overpotential cannot be used in the system of hydride electrodes.

Acknowledgements

This project was supported by the National Natural Foundation of China under contract No. 59701005.

References

[1] T. Sakai, H. Miyamura, N. Kuriyama, A. Kato, K. Oguro, H. Ishikawa, J. Electrochem. Soc. 137 (1990) 795.
[2] C.S. Wang, Y.Q. Lei, Q.D. Wang, Electrochim. Acta 43 (1998) 3193.
[3] M. Martin, C. Gommel, C. Borkhart, E. Fromm, J. Alloys Compd. 238 (1996) 193.
[4] J.J.G. Willems, Philips J. Res. 39 (1) (1984) 1.
[5] J.J.G. Willems, K.H.J. Buschow, J. Less-Common Met. 129 (1987) 13.
[6] M.A. FetCenko, S. Venkatesan, K.C. Hong, B. Reichman, in: Proceeding of the 16th International Power Source Symposium, vol. 12, International Power Source Committee, UK, 1983, p. 411.
[7] J.R.G.C.M. van Beek, J.J.G. Willems, H.C. Donkersloot, in: L.J. Pearce (Ed.), Proc. 14th Power Source Symp., 10, Power Sources, Brighton, 1985, p. 317.
[8] T. Sakai, H. Miyamura, N. Kuriyama, A. Kato, K. Oguro, H. Ishikawa, C. Iwakura, J. Less-Common Met. 159 (1990) 127.
[9] T. Sakai, K. Oguro, H. Miyamura, N. Kuriyama, A. Kato, H. Ishikawa, C. Iwakura, J. Less-Common Met. 161 (1990) 193.
[10] T. Sakai, T. Hazama, H. Miyamura, N. Kuriyama, A. Kato, H. Ishikawa, J. Less-Common Met. 172-174 (1991) 1175.
[11] T. Sakai, H. Yoshinaga, H. Miyama, N. Kuriyama, H. Ishikawa, J. Alloys Compd. 180 (1992) 3.
[12] M.P.S. Kumar, W. Zhang, K. Petrov, A. Rostami, S. Srinivasan, G.D. Adzic, J.J. Reilly, H.S. Lim, J. Electrochem. Soc. 142 (1995) 3424.
[13] D. Chartouni, F. Meli, A. Zuttel, K. Gross, L. Schlapbach, J. Alloys Compd. 241 (1996) 160.
[14] J.M. Cocciantlia, P. Bernard, S. Fernandez, J. Atain, J. Alloys Compd. 253–254 (1997) 642.
[15] G.D. Adzic, J.R. Johnson, S. Mukerjee, J. McBreen, J.J. Reily, J. Alloys Compd. 253–254 (1997) 579.
[16] P. Bernard, J. Electrochem. Soc. 145 (1997) 456.
[17] C. Iwakura, K. Fukuda, H. Senoh, H. Inoue, M. Matsuoka, Y. Yamamoto, Electrochem. Acta 43 (1998) 2041.
[18] P.H.L. Notten, P. Hokkeling, J. Electrochem. Soc. 138 (1991) 1877.
[19] G. Zheng, B.N. Popov, R.E. White, J. Electrochem. Soc. 142 (1995) 2695.
[20] Chunsheng Wang, J. Electrochem. Soc. 145 (1998) 1801.
[21] H.W. Yang, Y.Y. Wang, C.C. Wan, J. Electrochem. Soc. 143 (1996) 429.

[22] Q.M. Yang, M. Ciureanu, D.H. Ryan, J.Q. Strom-Olsen, J. Electrochem. Soc. 141 (1991) 2108.
[23] D. Lupu, A.R. Biris, J. Alloys Compd. 233 (1996) 192.
[24] M. Matsuoka, K. Asai, C. Iwakura, Electrochem. Acta 39 (1993) 659.
[25] H. Pan, Y. Chen, C. Wang, C.P. Cheng, Q. Wang, Electrochem. Acta 44 (1999) 2263.